# An Optimal State Dependent Haptic Guidance Controller Via a Hard Rein

Anuradha Ranasinghe
Department of Informatics
King's College London
London, United Kingdom
anuradha.ranasinghe@kcl.ac.uk

Jacques Penders
Sheffield Centre for Robotics
Sheffield Hallam University
Sheffield, United Kingdom
j.penders@shu.ac.uk

Kaspar Althoefer
Department of Informatics
Kings College London
London, United Kingdom
kaspar.althoefer@kcl.ac.uk

Prokar Dasgupta
Urology Centre MRC Centre for Transplantation
Kings College London
London, United Kingdom
Prokar.dasgupta@kcl.ac.uk

Thrishantha Nanayakkara
Department of Informatics
Kings College London
London, United Kingdom
thrish.antha@kcl.ac.uk

*Abstract*—The aim of this paper is to improve the optimality and accuracy of techniques to guide a human in limited visibility & auditory conditions such as in fire-fighting in warehouses or similar environments. At present, teams of breathing apparatus (BA) wearing fire-fighters move in teams following walls. Due to limited visibility and high noise in the oxygen masks, they predominantly depend on haptic communication through reins. An intelligent agent (man/machine) with full environment perceptual capabilities is an alternative to enhance navigation in such unfavorable environments, just like a dog guiding a blind person. This paper proposes an optimal state-dependent control policy to guide a follower with limited environmental perception, by an intelligent and environmentally perceptive agent. Based on experimental systems identification and numerical simulations on human demonstrations from eight pairs of participants, we show that the guiding agent and the follower experience learning for a optimal stable state-dependent a novel $3^{rd}$ and $2^{nd}$ order auto regressive predictive and reactive control policies respectively. Our findings provide a novel theoretical basis to design advanced human-robot interaction algorithms in a variety of cases that require the assistance of a robot to perceive the environment by a human counterpart.

*Index Terms*—Human robot interaction (HRI), Haptic, Optimal control policy, Predictive & reactive controllers

## I. INTRODUCTION

Literature on the subject of human-robot interaction (HRI) in low-visibility is rather sparse. There have been some studies on guiding people with visual and auditory impairments using intelligent agents in cases such as fire fighting [1] and guiding blind people using guide dogs [2]. Jacques & the team propose a swarm robotic approach with ad-hoc network communication to direct the fire fighters [1]. The main disadvantage of this approach is lack of bi-directional communication estimate the behavioral and psychological state of the firefighters. Personal navigation system using Global Positioning System (GPS) and magnetic sensor were used to guide blind people by Marston [2]. One major drawback with this approach is, upon arriving at a decision making point, the user has to depend on ges-ture based visual communication with the navigation support system, which may not work in low visibility conditions. Moreover, the acoustic signals used by the navigation support system may not suit noisy environments.

Another robot called Rovi, with environment perception capability has been developed to replace a guide dog [3]. Rovi had digital encoders based on retro-reflective type infra red light that recorded errors with ambient light changes. Though Rovi could avoid obstacles and reach a target on a smooth indoor floor, it suffers from disadvantages in uncertain environments. An auditory navigation support system for the blind is discussed in [4], where, visually impaired human participants (blind folded participants) were given verbal commands by a speech synthesizer. However, speech synthesis is not a good choice to command a visually impaired person in a stressful situation like a real fire. A guide cane without acoustic feedback was developed by Ulrich in 2001 [5]. The guide cane analyzes the situation and determines appropriate direction to avoid the obstacle, and steers the wheels without requiring any conscious effort [5]. Perhaps the most serious disadvantage of this study is that it does not take feedback from the visually impaired follower. To the best of our knowledge, there has been no detailed characterization of the bi-directional communication for guiding the person with a limited perception in a hazardous environment.

Recent studies were conducted on complementary task specialization [6] between a human-human pair and a human-robot pair to achieve a cooperative goal. It suggested that complementary task specialization develops between the human-human haptic negotiation process but not in the human-robot haptic interaction process [7]. This indicates that there are subtle features that should be quantified in the closed loop haptic interaction process between a human pair in task sharing. Haptic guidance has been found to be a very efficient way to train human subjects to make accurate 3D tracking movements

[8]. In [8]. Given the findings that human-human haptic cooperation obey certain characteristic optimality criteria like minimum jerk, optimal impedance control of the muscles & etc [9]. Therefore, characterization of human-human interaction in a haptic communication scenario, where one partner is blindfolded (limited perception of the environment) while the other human participant has fully perceptual capabilities, can provide a viable basis to design optimal human-robot interaction algorithms to serve humans working in many hazardous/uncertain environments. Therefore, this is the first paper to characterize the closed loop state dependent control policies of an agent with full perception capabilities & the blindfolded human.

The rest of the paper is organized as follows. Section II elaborates the experimental methodology to collect data of human-human interaction via a hard rein while tracking an arbitrary path. Section III describes the mathematical model of the guider's & the follower's state dependent control policies in detail. Section IV gives the experimental results of human participants along with numerical simulation results to show the stability of the control policies identified through experiments on human participants. It also discusses the virtual time varying damped initial model of the visually limited follower. Finally, section V gives a conclusion and future works.

## II. EXPERIMENTAL METHODOLOGY

Figure 1(A) shows how the guider and the blindfolded followers held both ends of hard rein to track the wiggly path so that the hard rein. For simplicity, hereafter we refer the follower" for the person with limited auditory & visual perception. We conducted the experiment to understand: 1) The guider's optimal state dependent control policy in an arbitrarily complex path, 2) The optimal control policy of the blindfolded followers, 3) whether the control policies of the guider & the follower are reactive controller or predictive controller.

In the experiment, eight pairs of subjects participated in the experiment after giving informed consent. They were healthy and in the age group of 23 - 43 years. One of the subjects (an agent with full perceptual capabilities) lead the other (a person with limited visual and auditory perceptions) using a hard rein as shown in figure 1(B). Visual feedback to the follower was cut off by blindfolding, while the auditory feedback was cut off by playing a sound track of less than 70dB as shown in figure 1(B). Figure 1(C) shows the relative orientation difference between the guider and the follower (referred to as state hereafter), and angle of the rein relative to the agent (referred to as action hereafter). MTx motion capture sensors (3-axis acceleration, 3-axis magnetic field strengths, 4-quaternions, 3-axis Gyroscope readings) were used to measure the states $\phi$ and actions $\theta$ of the duo. Two MTx sensors were attached on the chest of the guider and the follower to measure the rate of change of the orientation difference between them (state of the duo). Another two motion trackers were attached on the hard rein to measure the angle of the rein relative to the sensor on the chest of the guider (action from the agent). Since we used four MTx sensors, we sampled data at 25Hz to stay
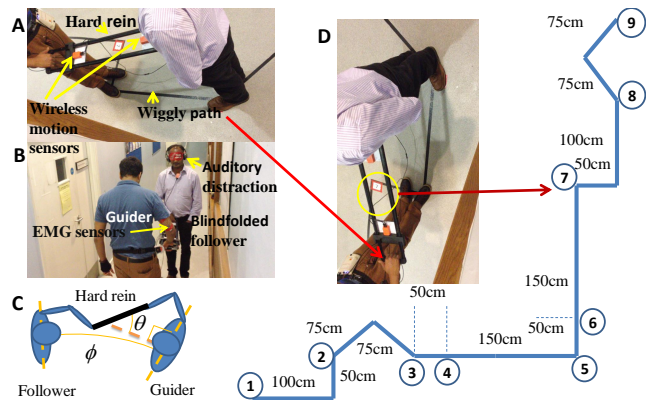


Fig. 1. The experimental setup: A) The hard rein with wireless MTx motion trackers. pushing/pulling in horizontal plane to guide the follower , B) Tracking the path by the duo, C) The hard rein with wireless MTx motion sensors attached to measure the state $\phi$ and the action $\theta$, D) The detailed diagram of labeled wiggly path on the floor

within hardware design limits. Four Electromyography (EMG) electrodes at 1500Hz were fixed on the guider's Anterior Deltoid, Biceps, Posterior Deltoid and lateral triceps along the upper arm as shown in figure 1(B). Before attaching EMG electrodes, the skin was cleaned with alcohol. For clarity, the detailed wiggly path is shown in figure 1(D). The path of total length 9m was divided into nine milestones as shown in figure 1(D). In any given trial, the guider was asked to take the follower from one milestone to another at six milestones up or down (ex. 1-7, 2-8, 3-9, 9-3, 8-2, and 7-1). The starting milestone was pseudo-randomly changed from trial to trial in order to eliminate the effect of any memory of the path. Moreover, the guider was disoriented before starting every trial. The guider was instructed to move the handle of the hard rein only on the horizontal plane to generate left and right turn commands. Furthermore, the guider was instructed to use push and pull commands for forwards and backwards movements. The follower was instructed to pay attention to the commands via hard rein to follow the guider. The follower started to follow the guider once a gentle tug was given via the rein. The experimental protocol was approved by the King's College London Biomedical Sciences, Medicine, Dentistry and Natural & Mathematical Sciences research ethics committee.

## III. MODELING

### A. The guider's closed loop control policy

We model the guider's control policy as an $N$-th order state dependent discrete linear controller. The order $N$ depends on the number of past states used to calculate the current action.

Let the state be the relative orientation between the guider and the follower given by $\phi$, and the action be the angle of the rein relative to the sensor on the chest of the guider given by $\theta$ as shown in figure 1(C). Then the linear discrete control policy of the guider is given by

$$\theta_g(k) = \sum_{r=0}^{N-1} a_r^{gRe} \phi_g(k-r) + c^{gRe} \qquad (1)$$

if it is a reactive controller, and

$$\theta_g(k) = \sum_{r=0}^{N-1} a_r^{gPre} \phi_g(k+r) + c^{gPre} \qquad (2)$$

if it is a predictive controller, where, $k$ denotes the sampling step, $N$ is the order of the polynomial, $a_r^{gRe}, a_r^{gPre}, r = 1, 2, \cdots, N$ is the polynomial coefficient corresponding to the $r$-th state in the reactive and predictive model respectively, and $c^{gRe}, c^{gRe}$ are corresponding scalars.

*B. The follower's closed loop control policy*

While the guider's control policy is represented by equations 1 and 2, we again model the follower's control policy as an $N$-th order action dependent discrete linear controller to understand behavior of the follower. The order $N$ depends on the number of past actions used to calculate the current state. Then the linear discrete control policy of the follower is given by

$$\phi_f(k) = \sum_{r=0}^{N-1} a_r^{fRe} \theta_f(k-r) + c^{fRe} \qquad (3)$$

if it is a reactive controller, and

$$\phi_f(k) = \sum_{r=0}^{N-1} a_r^{fPre} \theta_f(k+r) + c^{fPre} \qquad (4)$$

if it is a predictive controller, where, $k$ denotes the sampling step, $N$ is the order of the polynomial, $a_r^{fRe}, a_r^{fPre}, r = 1, 2, \cdots, N$ is the polynomial coefficient corresponding to the $r$-th state in the reactive and predictive model respectively, and $c^{fRe}, c^{fPre}$ are corresponding scalars. These linear controllers in equations 1,2, 3 and 4 can be regressed with the experimental data obtained in the guider-follower experiments above to obtain the behavior of the polynomial coefficients across trials. The behavior of these coefficients for all human participants across the learning trials will give us useful insights as to the predictive/reactive nature, variability, and stability of the control policy learned by human guiders. Furthermore, a linear control policy given in equations 1, 2, 3 and 4 would make it easy to transfer the fully learned control policy to a robotic guider in a low visibility condition.

*C. Modeling the follower as a virtual time varying damped initial system*

In order to study how the above control policy would interact with the follower in an arbitrary path tracking task, we model the blindfolded human participant (follower) as a damped inertial system, where a force $F(k)$ applied along relative to the follower's heading direction at sampling step $k$ would result in a transition of position given by $F(k) = M\ddot{P}_f(k) + \zeta \dot{P}_f(k)$, where $M$ is the virtual mass, $P_(f)$ is the position vector in the horizontal plane, and $\zeta$ is the virtual damping coefficient. It should be noted that the virtual mass and damping coefficients are not those real coefficients of the follower's stationary body, but the mass and damping coefficients felt by the guider while the duo is in voluntary

movement. This dynamic equation can be approximated by a discrete state-space equation given by

$$x(k) = Ax(k-1) + Bu(k) \qquad (5)$$

where , $x(k) = \begin{bmatrix} P_f(k) \\ P_f(k-1) \end{bmatrix}, x(k-1) = \begin{bmatrix} P_f(k-1) \\ P_f(k-2) \end{bmatrix},$

$A = \begin{bmatrix} (2M+T\zeta)/(M+T\zeta) & -M/(M+T\zeta) \\ 1 & 0 \end{bmatrix},$

$\mathrm{B} = \begin{bmatrix} T^2/(M+T\zeta) \\ 0 \end{bmatrix}, u(k) = F(k),$

$k$ is the sampling step & T is the sampling time.

Given the updated position of the follower $P_f(k)$, the new position of the guider $P_g(k)$ can be easily calculated by imposing the constraint $\|P_f(k) - P_g(k)\| = L$, where $L$ is the length of the hard rein.

## IV. EXPERIMENTAL RESULTS

We conducted experiments with human participants to understand how the coefficients of the control policy relating states $\phi$ and actions $\theta$ given in equations 1, 2, 3, and 4 settle down across learning trials. In order to have a deeper insight into how the coefficients in the discrete linear controller in equations 1, 2, 3, and 4 change across learning trials, we ask 1) whether the guider and the follower tend to learn a predictive/reactive controllers across trials, 2) whether the order of the control policy of the guider in equations 1 & 2 and the order of the control policy of the follower in equations 3 & 4 change over trials, and if so, what its steady state order would be.

To find regression coefficients, since the raw motion data were contaminated with noise, we use the 4th decomposition level of Daubechies wave family in Wavelet Toolbox (The Math Works, Inc) for the state and the action profiles for regression analysis. Since the guider generates swinging actions in the horizontal plane, the Daubechies wave family best suits such continuous swing movements [10].

*A. Determination of the salient features of the guider's control policy*

First, we used experimental data for action $\theta$ and state $\phi$ in equations 1 and 2. Once the coefficients of the polynomial in equations 1 and 2 are estimated, the best control policy (equations 1 or 2), and the corresponding best order of the polynomial should give the best $R^2$ value for a given trial across all subjects. To select best fit policies, coefficients of (equations 1 are 2) were estimated from $1^{st}$ order to $4^{th}$ order polynomials shown in figure 2 (A). Dashed line and solid line were used to denote reactive and predictive models respectively. Twenty trials were binned to five for clarity. From figure 2 (A), we can notice that the $R^2$ values corresponding to the $1^{st}$ order model in both equations 1 and 2 are the lowest. The relatively high $R^2$ values of the higher order models suggest that the control policy is of order $> 1$. Therefore, we take the % differences of $R^2$ values of higher order polynomials relative to the $1^{st}$ order polynomial for both equations 1 and 2 to assess the fitness of the predictive control policy given in equation
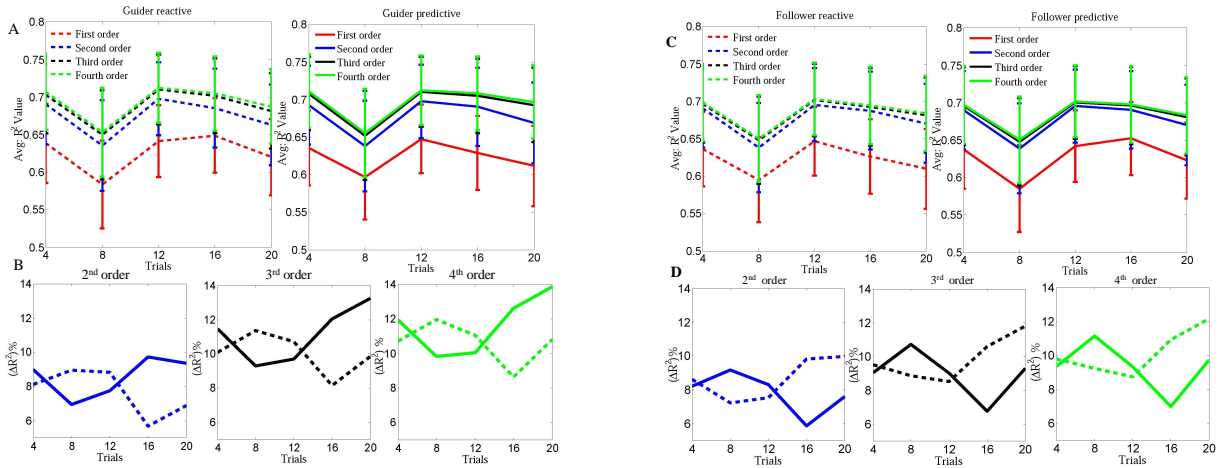
Fig. 2. $R^2$ values from $1^{\text{st}}$ order to $4^{\text{th}}$ order polynomials for the guider and the follower: reactive models (dashed line) and predictive models (solid line): (A) & (C) are the $R^2$ value variation of the reactive and predictive from $1^{\text{st}}$ to $4^{\text{th}}$ order polynomials over trials for the guider & the follower respectively. (B) & (D) are the % differences of $R^2$ values of $2^{\text{nd}}$ to $4^{\text{th}}$ order polynomials with respect to 1st order polynomial for the guider's & the follower's control policies respectively: $2^{\text{nd}}$ order (blue), $3^{\text{rd}}$ order (black), $4^{\text{th}}$ order (green).

2 relative to the reactive policy given in equation 1. Figure 2 (B) shows that the marginal % gain in $R^2$ value ($\triangle R^2\%$) of $2^{\text{nd}}$, $3^{\text{rd}}$, and $4^{\text{th}}$ order polynomials in equation 2 (predictive control policy) grows compared (solid line) to those of the reactive control (dashed line) policy in equation 1. Therefore, we conclude that the guider gradually gives more emphasis on a predictive control policy than a reactive one. The percentage (%) gain of of $3^{\text{rd}}$ order polynomial is highest campared to $2^{\text{nd}}$ & $4^{\text{th}}$ order polynomials as shown in table I by numerical values & the figure 2 (B). There is a statistically significant improvement from $2^{\text{nd}} \rightarrow 3^{\text{rd}}$ order models ( $p < 0.03$), while there is not significant information gain from $3^{\text{rd}} \rightarrow 4^{\text{th}}$ order models ( $p > 0.6$ ). It means that the guider predictive control policy is more explained when the order is $N = 3$. Therefore, hereafter, we consider $3^{\text{rd}}$ order predictive control policy to explain the guider's control policy.

TABLE I
GUIDER PREDICTIVE $\triangle R^2\%$ OF $2^{\text{nd}}$ TO $4^{\text{th}}$ ORDER POLYNOMIALS W.R.T $1^{\text{st}}$ ORDER

| Trial No: | $2^{\text{nd}}$ order | $3^{\text{rd}}$ order | $4^{\text{th}}$ order | $p$ values |
|---|---|---|---|---|
| 4 | 8.99 | 11.44 | 11.95 | |
| 8 | 6.95 | 9.28 | 9.84 | |
| 12 | 7.75 | 9.70 | 10.06 | $p_{(2^{nd}\leftrightarrow 3^{rd})} < 0.03*$, |
| 16 | 9.74 | 12.04 | 12.61 | $p_{(3^{rd}\leftrightarrow 4^{th})} > 0.6$ |
| 20 | 9.35 | 13.26 | 13.87 | |

### B. Determination of the salient features of the follower's control policy

Next our attempt is to understand the salient features of the follower's control policy. We used experimental data for state $\theta$ and action $\phi$ in equations 3 and 4 to extract features of the follower's control policy from $1^{\text{st}}$ to $4^{\text{th}}$ order polynomials over trials as shown in figure 2 (C). Here, we used same

TABLE II
FOLLOWER REACTIVE $\triangle R^2\%$ OF $2^{\text{nd}}$ TO $4^{\text{th}}$ ORDER POLYNOMIALS W.R.T $1^{\text{st}}$ ORDER

| Trial No: | $2^{nd}$ order | $3^{rd}$ order | $4^{th}$ order | $p$ values |
|---|---|---|---|---|
| 4 | 8.60 | 9.52 | 9.79 | |
| 8 | 7.23 | 8.87 | 9.23 | |
| 12 | 7.54 | 8.51 | 8.74 | $p_{(2^{nd}\leftrightarrow 3^{rd})} > 0.1$, |
| 16 | 9.81 | 10.59 | 10.92 | $p_{(3^{rd}\leftrightarrow 4^{th})} > 0.7$ |
| 20 | 9.99 | 11.81 | 12.16 | |

mathematical & statistical method as guider's model. Interestingly, figure 2 (C) shows that the marginal % gain in $R^2$ value ($\triangle R^2\%$) of $2^{\text{nd}}$, $3^{\text{rd}}$, and $4^{\text{th}}$ order polynomials in equation 3 (reactive control policy) grows compared (dashed line) to those of the predictive control (solid line) policy in equation 4. Therefore, we conclude that the follower gradually gives more emphasis on a reactive control policy than a predictive one. Again here, we tried to find the best fit order to explain the follower's control policy. The percentage (%) gain of of $2^{\text{nd}}$ order polynomial is highest compared to $3^{\text{rd}}$ & $4^{\text{th}}$ order polynomials as shown in table II by numerical values & the figure 2 (D). Interestingly, There is no statistically significant improvement from $2^{\text{nd}} \rightarrow 3^{\text{rd}}$ order models ( $p > 0.1$) nor from $3^{\text{rd}} \rightarrow 4^{\text{th}}$ order models ( $p > 0.7$ ). Therefore, we can say the follower reactive control policy is more explained when the order is $N = 2$. Therefore, hereafter, we consider $2^{\text{nd}}$ order reactive control policy to explain the follower's control policy.

### C. Polynomial parameters of a novel linear state dependent controllers of the duo

Then we move into understand how the polynomial parameters of a $3^{\text{rd}}$ & $2^{\text{nd}}$ order linear state dependent controllers would evolve across learning trials in equation 2 & 3 for the guider & the follower respectively. We notice in figure 3 & 4 that the history of the polynomial coefficients fluctuates within
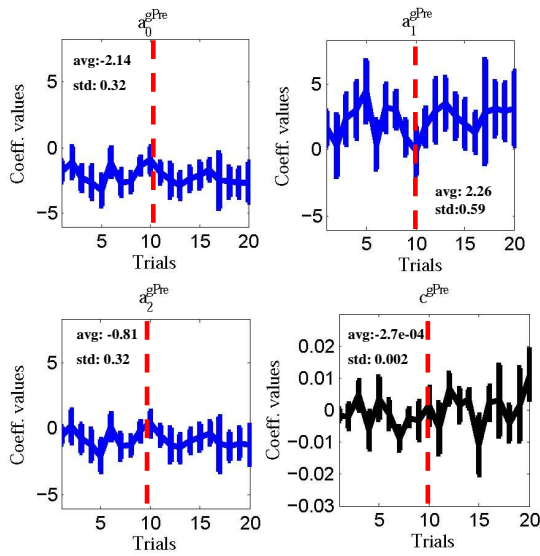
Fig. 3. The evolution of coefficients of the $3^{rd}$ order auto regressive predictive controller of the guider.
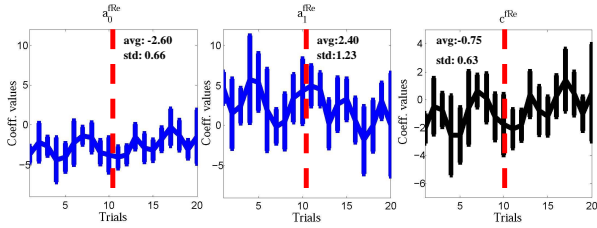


Fig. 4. The evolution of coefficients of the $2^{nd}$ order auto regressive reactive controller of the follower.

bounds for both the guider predictive & the follower reactive. (The average & S.D values of the coefficients are labeled). This could come from the variability across participants and variability of the parameters across trials itself. Therefore, we estimate the above control policy as a bounded stochastic decision making process.
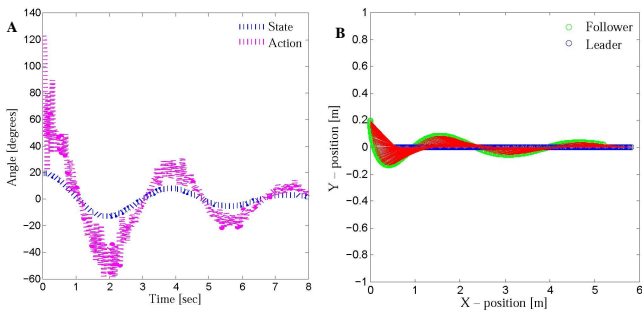


Fig. 5. Simulation results: (A)The behavior of the state and the action for the simulated guider-follower scenario. The control policy was based on the coefficients extracted from the experiments on human participants.(B) Stable behavior of trajectories of the follower (green) for where the guider tries to get the follower to move along a straight line from a different initial location. The control policy was based on the coefficients extracted from the experiments on human participants.

## D. Developing a closed loop path tracking controller with a simulator

Back to our main problem is to guide a person with visually and auditory limited perception of the environment by using another (human or machine) who with full perceptual capabilities. Our $3^{rd}$ order auto regressive control policy explains more human guider behavior. Furthermore, if we could combine our experimental results with a simulator, it would be a complete solution for our problem.

We use the last 10 trials coefficients values as marked on figure 3 & 4 by red dashed line to calculate the statistical features of the regression coefficients in order to make sure the model reflects the behavior of the human participants at a mature learning stage. The model parameters were then found to be: $a_0 = N(-2.3152, 0.2933^2)$, $a_1 = N(2.6474, 0.5098^2)$, $a_2 = N(2.6474, 0.5098^2)$ and $c = N(1.0604e - 04, 0.2543^2)$.

In order to ascertain whether the control policy obtained by this systems identification process is stable for an arbitrarily different scenario, we conducted numerical simulation studies forming a closed loop dynamic control system of the guider and the follower using the control policy given in equation 2 together with the discrete state space equation of the follower dynamics given in equation 5. The length of the hard rein $L = 0.5$m, the follower's position $P_f(0)$ was given an initial error of 0.2m at $\phi(0) = 45°$, the mass of the follower $M = 10$[kg] with the damping coefficient $\zeta = 4$[Nsec/m], the magnitude of the force exerted along the rein was 5N, and the sampling step $T = 0.02$.

From figure 5(B) we notice that the follower asymptotically converges to the guider's path within a reasonable distance. The corresponding behavior of the state and the resulting control action shown in figure 5 (A) further illustrates that the above control policy can generate bounded control actions given an arbitrary error in the states.

Then we go back to the original experimental data of the human participants to ask whether the responsibility assignment among the muscles and the total energy consumed to implement the control policy changed across the trials.

In order to ascertain whether the low internal impedance control strategy converges to a minimum energy control solution, how does the individual muscle EMG vary over trials? To find the answer, we plotted average normalized individual muscle over trials as shown in figure 6 (A). EMG signals were amplified and filtered according to standard method [11]. We notice that the proportion of responsibility taken by the posterior Deltoid monotonically increases relative to the anterior Deltoid. Moreover, proportion of responsibility taken by the Biceps increases relative to the Triceps. This indicates that the above muscle pairs try to reduce co-activation in order to learn a low internal impedance control strategy. Therefore, this is in agreement with other studies that show a similar pattern of reduction in muscle co contraction when motor learning progresses [12]. Next, we further analyzed the behavior of the averaged normalized EMG ratio between frontal and dorsal muscles as shown if figure 6 (B). The ratio of anterior and posterior muscles are decreased over trials in figure 6 (B):
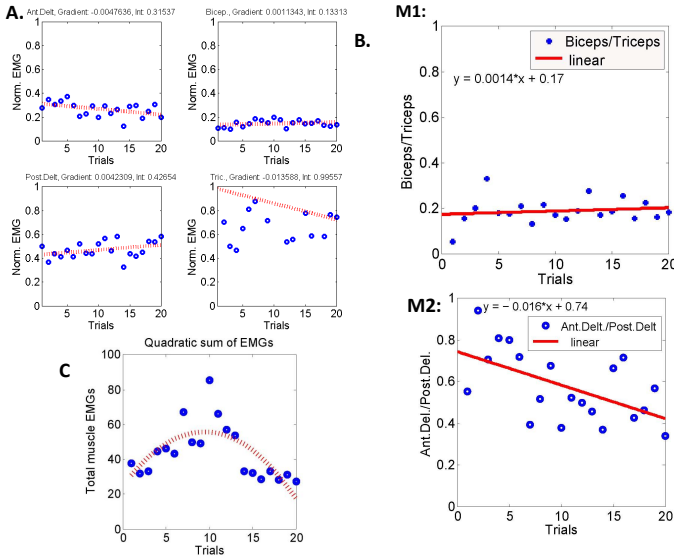
Fig. 6. The behavior of the average normalized muscle EMGs: (A)Average normalized muscle EMG anterior Deltoid, posterior Deltoids, Biceps, and Triceps.(B) Frontal and dorsal muscle ratio: M1- Biceps triceps muscle ratio, M2- anterior Deltoid posterior Deltoid muscle ratio. (C) The behavior of this cost indicator $J$ of the $2^{nd}$ order best fit curve for average EMGs of all four muscles of the eight subjects across trials.

M1 while ratio of Biceps and Triceps is increased in figure 6 (B): M2. This suggests that, the priority muscle activation is taken by frontal and dorsal muscle of Deltoid than Biceps Triceps pair while the guiding agent produces movements in horizontal plane swing, anterior and posterior Deltoid pair is more activated to generate the tug forces along the hard rein. Alternatively, to compute the average EMG for all four muscles of all eight participants that reflects the average energy consumed in a trial given by $J = \sqrt{\sum_{i=1}^{4} \sum_{j=1}^{S_N} EMG_{ij}^2}$, where $S_N$ is the number of subjects, $EMG_{ij}$ is the average rectified EMG of the $i$th muscle of the $j$th participant (guiding agent). The behavior of this cost indicator $J$ is shown in figure 6 (C). We can clearly observe from the 2nd order best fit curve that $J$ starting from lower- mid way of the training trials increase to a maximum - decreases in last 10 trials - reaches to minimum values at the last trial. This suggests that optimization is a non-monotonic process. During the first trials, it may have given priority to order selection than optimization in the actuation space, which is also reflected in the behavior of $R^2$ values in figure 2. Once the optimal order is selected, subjects exhibit monotonic optimization in the actuation space as seen in the last 10 trials of figure 6(C), with a corresponding increase of $R^2$ values in figure 2.

## V. CONCLUSION AND FUTURE WORKS

This study was conducted to understand how two human participants interact with each other using haptic signals through a hard rein to achieve a path tracking goal when one partner (the follower) is blindfolded, while the other (the guider) gets full state feedback of the follower. We found that 1) the control policy of the guider & the follower can be approximated by a $3^{rd}$ & $2^{nd}$ order auto-regressive models respectively, 2) while the guider develops a predictive controller, the follower gradually develops reactive controllers across learning trials. The cost functions that are minimized by the duo, during learning to track a path, we found that the guider gradually progresses from an initial muscle co-contraction based command generation strategy to a low energy policy with minimum muscle co-contraction[13].

In addition to applications in robotic guidance of a person in a low visibility environment, our findings shed light on human-robot interaction applications in other areas like robot-assisted minimally invasive surgery (RMIS). Surgical tele-manipulation robot could use better predictive algorithms to estimate the parameters of remote environment for the surgeon with more accurate adaption of control parameters by constructing internal models of interaction dynamics between tools and tissues in order to improve clinical outcomes.

## REFERENCES

[1] J. Penders et al. , "A robot swarm assisting a human firefighter", *Advanced Robotics*, vol 25, pp.93-117, 2011.
[2] J. R. Marston et al, "Nonvisual route following with guidance from a simple haptic or auditory display", *Journal of Visual Impairment & Blindness*, vol.101(4), pp.203-211, 2007.
[3] A. A.Melvin et al, "ROVI: a robot for visually impaired for collision-free navigation ",*Proc. of the International Conference on Man-Machine Systems (ICoMMS 2009)*, pp. 3B5-1-3B5-6, 2009.
[4] J. M. Loomis et al, "Navigation system for the blind: Auditory Display Modes and Guidance", *IEEE Transaction on Biomedical Engineering*, vol.7, pp. 163 - 203, 1998.
[5] I. Ulrich and J. Borenstein, "'The GuideCane-applying mobile robot technologies to assist the visually impaired ",*Systems, Man and Cybernetics, Part A: Systems and Humans, IEEE Transactions*, vol. 31, pp. 131 - 136, 2001.
[6] K. B. Reed et al "Haptic cooperation between people, and between people and machines", *IEEE/RSJ Int. Conf. on Intelligent Robots and Systems (RSJ)*, vol. 3, pp. 2109-2114, 2006.
[7] K. B. Reed et al, "Replicating Human-Human Physical Interaction", *IEEE International Conf. on Robotics and Automation (ICRA)*, vol.10, pp. 3615 - 3620, 2007.
[8] D. Feygin et al, "Haptic Guidance:Experimental Evaluation of a Haptic Training Method for a perceptual Motor Skill", *Proc. of the 10th symp. on haptic interferences for Virtual Enviornment and Teleoperator systems(HAPTICS 2002)*, pp. 40 - 47, 2002.
[9] K. B. Reed et al "'Haptic cooperation between people, and between people and machines'", *In IEEE/RSJ Int. Conf. on Intelligent Robots and Systems*, pp. 2109-2114, 2006.
[10] Flanders.M, "Choosing a wavelet for single-trial EMG" „*Journal of Neuroscience Methods*, vol.116.2, pp.165-177, 2002.
[11] Flanders et al, "Basic features of phasic activation for reaching in vertical planes",*Experimental Brain Research*, vol.110, pp. 67-79, 1996.
[12] D.W. Franklin et al. "Adaptation to stable and unstable dynamics achieved by combined impedance control and inverse dynamics model" „*Journal of neurophysiology*,vol.90, pp. 3270-3282,2003.
[13] K.A. Thoroughman and S. Reza. "Learning of action through adaptive combination of motor primitives" ,*Nature*, vol.407, pp. 742-747,2000.